IL NUOVO CIMENTO **39 C** (2016) 318
DOI 10.1393/ncc/i2016-16318-6

Colloquia: La Thuile 2016

The JUNO experiment

C. Jollet on behalf of JUNO Collaboration
Université de Strasbourg, IPHC - Strasbourg, France

received 26 July 2016

Summary. — The Jiangmen Underground Neutrino Observatory (JUNO) is a large liquid scintillator detector aiming at the measurement of anti-neutrinos issued from nuclear reactors at a 53 km distance, having as primary goal the determination of the neutrino mass hierarhcy. The detector will be located 1800 m.w.e. underground and consists of a 20 kiloton liquid scintillator contained in a 35.4 m diameter acrylic sphere, instrumented by more than 17000 20 inch PMTs ensuring a 77% photocatode coverage. The required energy resolution to discriminate between the hierarchies at the 3–4 σ C.L. in about 6 years of data taking is 3% at 1 MeV. To achieve such a precision, severe constraints on the detector components quality are set: the PMTs need a quantum efficiency of more than 27% and the attenuation length of the liquid has to be better than 20 m (at 430 nm). The precise measurement of the anti-neutrino spectrum will allow to reduce the uncertainty below 1% on solar oscillation parameters. The international collaboration of JUNO was established in 2014, the civil construction started in 2015 and the R&D of the detectors is ongoing. The expected start of data taking is set for 2020.

1. – Introduction

The discovery of a non-zero value of the θ_{13} mixing angle [1-3] opened the way for the CP violation search in the leptonic sector, which is indeed the major goal of the next-generation long-baseline neutrino experiments [4]. An additional goal for the next generation of neutrino experiments is the determination of the mass hierarchy (MH). Different approaches are considered: long-baseline (order of 1000 km) experiments which exploit the matter effects on the oscillation probability [4,5], huge Cherenkov detectors to observe the zenith angle *versus* energy pattern in atmospheric neutrino oscillations [6,7], and medium-baseline (order of 50 km) reactor anti-neutrino experiments [8, 9] which observe the fast oscillations driven by θ_{13} on top of the solar ones.

The Jiangmen Underground Neutrino Observatory (JUNO) is a multipurpose neutrino experiment, which has indeed as primary goals the determination of the mass hierarchy using reactor anti-neutrinos [8]. The experiment geographical location is shown in fig. 1: the underground laboratory will be located at Jiangmen, with a rock overburden

Cores	YJ-C1	YJ-C2	YJ-C3	YJ-C4	YJ-C5	YJ-C6
Power (GW)	2.9	2.9	2.9	2.9	2.9	2.9
Baseline (km)	52.75	52.84	52.42	52.51	52.12	52.21
Cores	TS-C1	TS-C2	TS-C3	TS-C4	DYB	HZ
Power (GW)	4.6	4.6	4.6	4.6	17.4	17.4
Baseline (km)	52.76	52.63	52.32	52.20	215	265

Fig. 1. – Location of the JUNO site. The distances to the nearby Yangjiang and Taishan nuclear power plants are both 53 km. Daya Bay nuclear power plant is 215 km away. In the inset the power and distance of the different cores from the detector are stated. The two of the four cores of Taishan nuclear power plant have been planned by the company, but the approval by the government is pending.

of about 700 m, at a distance of 53 km away from the Taishan and Yangjiang reactor complexes.

2. – Mass hierarchy sensitivity

The mass hierarchy gives the order of neutrino masses and we have two cases: normal hierarchy (NH) for $\nu_1 < \nu_2 < \nu_3$ or inverted hierarchy (IH) for $\nu_3 < \nu_1 < \nu_2$. The hierarchy is nowadays still unknown since the measurements of the so-called atmospheric mass splitting ($\Delta m^2_{atm} \approx \Delta m^2_{31} \approx \Delta m^2_{32}$) resulted in an absolute value of such a parameter but the sign could not be determined yet. This is indeed one of the main goals of the JUNO experiment.

If we look at the spectrum of reactor antineutrinos expected at the JUNO detector (see fig. 2) we see that the main oscillation ($\bar{\nu_e} \to \bar{\nu_x}$) is driven by the solar terms. On top of that small wiggles are clearly visible, representing the θ_{13} driven oscillation: the pattern is different in case of NH and IH.

The antineutrino spectrum contains therefore the MH information: the sensitivity can be evaluated using a χ^2-function and the MH discriminator can be defined as

$$\Delta\chi^2_{MH} = |\chi^2_{min}(NH) - \chi^2_{min}(IH)|. \tag{1}$$

An alternative way to determine the mass hierarchy is to apply a Fourier analysis on the reconstructed energy spectrum as explained in ref. [10]. Using the positions of "peaks" and "valleys" found in the sine and cosine Fourier transforms (see, *e.g.*, fig. 3), some observables can be defined and used to assess the MH.

Two critical parameters have to be optimized, namely the baseline and the energy resolution. The final sensitivity on the MH discrimination is indeed quickly reduced when

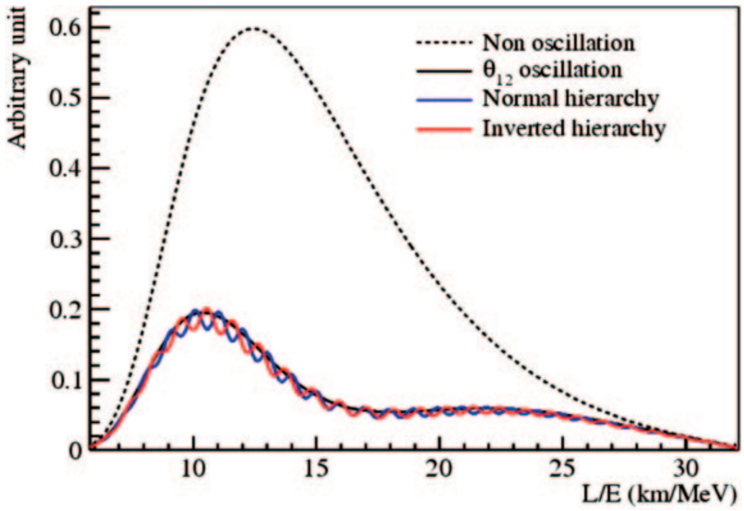

Fig. 2. – Expected antineutrino spectrum in terms of L/E. The dashed line gives the non-oscillated spectrum, the solid black line correspond to the spectrum after solar-driven (mixing angle θ_{12}) oscillation whereas the blue and red solid lines corresponds to the θ_{13} driven oscillations for NH and IH, respectively.

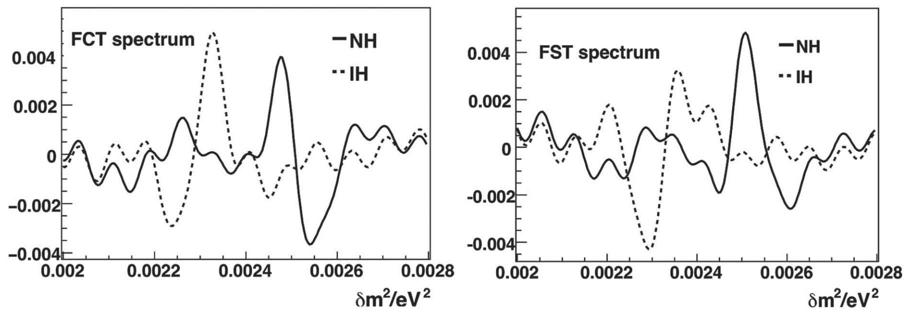

Fig. 3. – Sine and cosine Fourier transform of the reconstructed energy spectrum. The "peaks" and "valleys" used to build the observables are clearly seen.

the energy resolution is degraded as can be seen in fig. 4. For this reason the experiment design goal is an energy resolution of $3\%/\sqrt{(E)}[\mathrm{MeV}]$.

The same is true for the baseline, which has to be set at $\sim 53\,\mathrm{km}$, with in addition a good control of the distance difference between the detector and the respective reactor cores. Such a difference should not exceed 500 m as clearly shown in fig. 5.

The measurement performed by JUNO can be performed in a relative way, *i.e.* assuming no constraints on Δm^2_{31} or Δm^2_{32}, or in a relative way taking into account constraints coming from other experiments, in particular long-baseline ones. Indeed, long-baseline neutrino experiments are typically sensitive to $\Delta m^2_{\mu\mu}$ which can be written as

$$\Delta m^2_{\mu\mu} \simeq \sin^2\theta_{12}\Delta m^2_{31} + \cos^2\theta_{12}\Delta m^2_{32} + \sin 2\theta_{12}\sin\theta_{13}\tan\theta_{23}\cos\delta\Delta m^2_{21}, \tag{2}$$

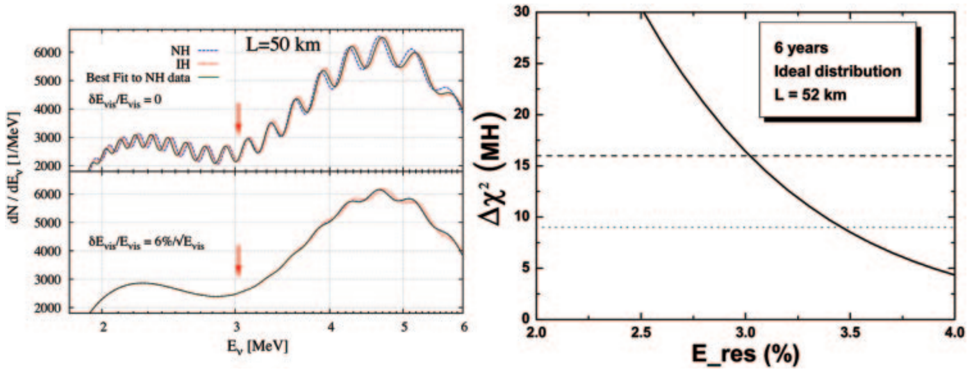

Fig. 4. – Left: reconstructed energy spectra with perfect energy resolution (top) and $6\%/\sqrt{(E)[\mathrm{MeV}]}$ (bottom). Right: MH sensitivity as a function of the energy resolution.

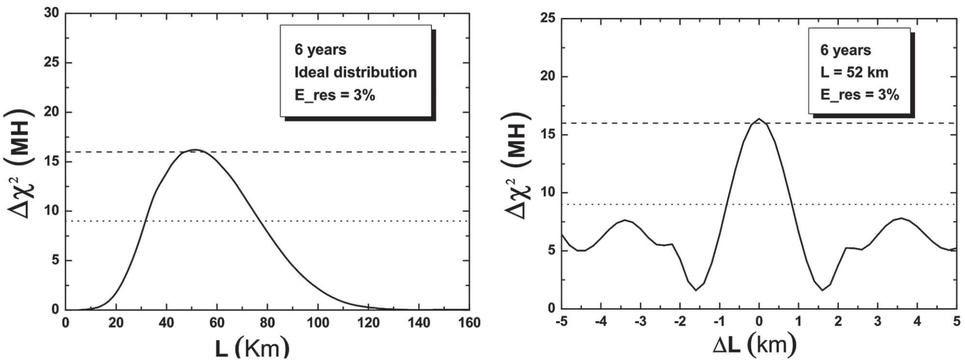

Fig. 5. – Left: MH sensitivity as a function of the distance between the detector and the reactor cores. Right: MH sensitivity as a function of the difference of distances between the detector and the respective reactor cores.

whereas reactor antineutrino experiments are sensitive to Δm^2_{ee} which can be written as

$$\Delta m^2_{ee} \simeq +\cos^2\theta_{12}\Delta m^2_{31} + \sin^2\theta_{12}\Delta m^2_{32}. \tag{3}$$

A constraint on $\Delta m^2_{\mu\mu}$ would therefore result in a better constraint on Δm^2_{ee} increasing the sensitivity on MH. The current precision on $\Delta m^2_{\mu\mu}$ is of about 4% but combining T2K [11] and NOvA [12] results we could have a precision of about 1% in 2020.

With 100k IBDs measured, the JUNO experiment will reach a $\Delta\chi^2 > 9$ for a MH relative measurement, and $\Delta\chi^2 > 16$ for an absolute measurement assuming 1% precision on $\Delta m^2_{\mu\mu}$, as can be seen in fig. 6.

3. – Detector design

The JUNO detector consists of a 35.4 m diameter acrylic sphere filled with 20 kton purified liquid scintillator. The scintillator is based on LAB (linear alkylbenzene) with an

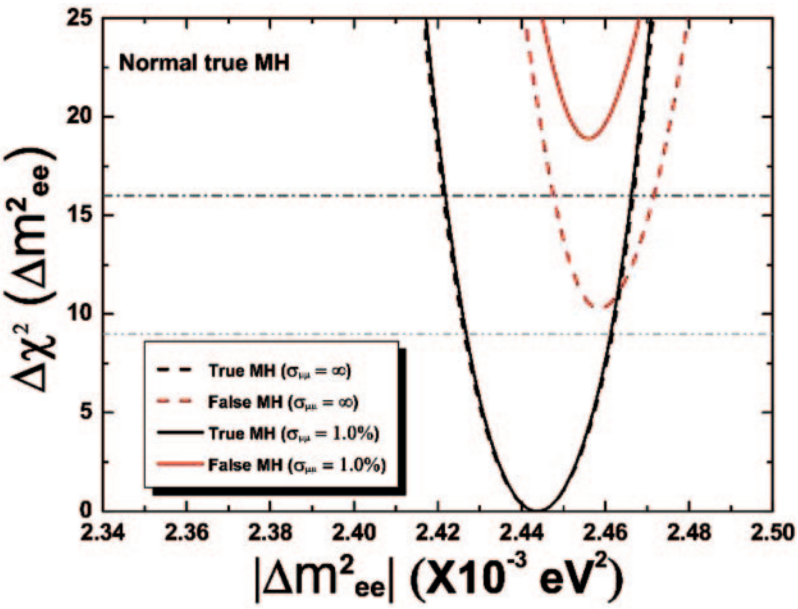

Fig. 6. – MH sensitivity for the relative and absolute measurement with 100k IBDs measured by JUNO.

attenuation lenght of more than 20 m doped with PPO (2,5-diphenyloxazole) as primary fluor and bis-MSB (p-bis-(o-methylstyryl)-benzene) as wavelength shifter. Contrarily to what was chosen for smaller experiments such as Double Chooz, the scintillator is Gd free in order to be more stable in time, reduce the radioactivity and maximise the attenuation length.

A stainless steel latticed shell sustained by more than 100 pillars will surround the acrylic sphere and support the ~ 17000 20″ PMTs and ~ 34000 3″ PMTs observing the neutrino target with a cathode coverage of about 77%. The 3″ PMTs will be installed in the gap between large PMTs and they will permit to improve the non-stochastic term of the energy resolution.

Two vetoes are foreseen to reduce the different sources of background. A 20 ktons ultrapure water Cherenkov pool around the central detector, instrumented by ~ 2000 20″ PMTs, will tag events coming from outside the neutrino target. It will also act as a passive shielding for neutrons and gammas. In addition a muon tracker will be installed on top of the detector (top muon veto) in order to tag cosmic muons and validate the muon track reconstruction. The top muon veto will use the OPERA experiment target tracker currently being decommissioned [13].

A schematic view of the detector can be seen in fig. 7

4. – Signal and background

The signal will be identified observing the inverse beta decay process, *i.e.* $\bar{\nu_e} + p \rightarrow e^+ + n$ relying on the twofold coincidence between the prompt signal given by the positron ionization and annihilation (1–10 MeV), and the delayed signal of 2.2 MeV given by the neutron capture on hydrogen ($\Delta t \sim 200\,\mu$s).

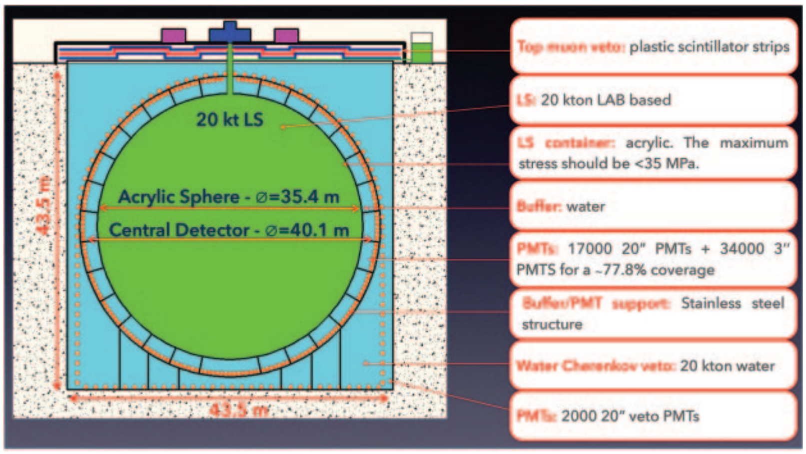

Fig. 7. – Schematic view of the JUNO detector.

Efficiency, signal and background rates after each selection criterion

Selection	IBD efficiency	IBD	Geo-νs	Accidental	^{9}Li/^{8}He	Fast n	(α, n)
-	-	83	1.5	$\sim 5.7 \times 10^4$	84	-	-
Fiducial volume	91.8%	76	1.4		77	0.1	0.05
Energy cut	97.8%			410			
Time cut	99.1%	73	1.3		71		
Vertex cut	98.7%			1.1			
Muon veto	83%	60	1.1	0.9	1.6		
Combined	73%	60	3.8				

Fig. 8. – Signal and background reduction table including the different cut efficiency [8].

The background is divided in accidental and correlated. The accidental is given by radioactivity gammas (typically from PMTs or surrounding rock) which fake a prompt or a delay signal, and it can be reduced with passive shielding. The correlated background is mostly given by cosmogenic isotopes such as ^{9}Li produced by muons in the detector. A good muon reconstruction is needed to reject them since a volume veto will be applied around the muon track for about 1.2 s. In addition fast neutrons produced by the muons in the surrounding rock could enter the detector faking the signal signature. To reject the neutrons passive shielding can be used as well as selections based on the detection of multiple proton recoils.

After the background rejection cuts, a signal of about 60 events per day is expected with a remaining background of about 3.8 events per day (see fig. 8).

5. – Schedule

The JUNO international collaboration was established in 2014, and data taking is foreseen to start in 2020. Civil construction is ongoing and the tunnel access to the underground laboratory is almost completed. A cartoon showing the overall JUNO schedule can be seen in fig. 9.

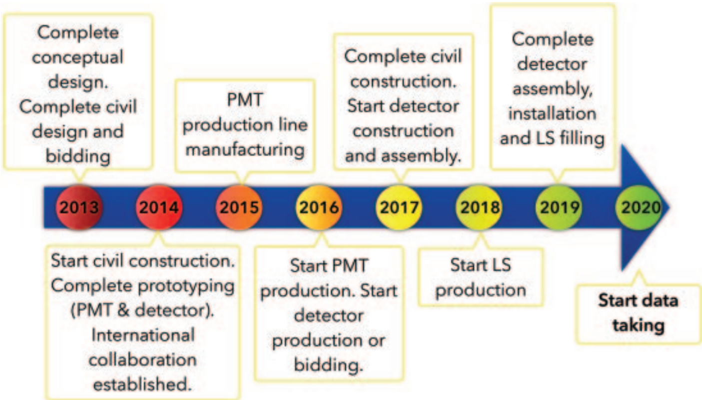

Fig. 9. – Cartoon showing the overall JUNO schedule.

6. – Conclusions

The JUNO experiment was approved in February 2013 and the international collaboration was established in 2014 with the goal of data taking in 2020.

The main goal of the experiment is the mass hierarchy determination and a sensitivity of $\Delta\chi^2 > 9$ (relative measurement) is expected with 6 years of data taking. If the knowledge at 1% is assumed on $\Delta m^2_{\mu\mu}$ the sensitivity is increased to $\Delta\chi^2 > 16$.

To reach this goal the JUNO design is an unprecedented large (20 kton) and high-precision calorimetry liquid scintillator requiring high transparency (20 m attenuation length), and high light collection (1200 p.e./MeV) to reach a 3% energy resolution at 1 MeV.

Besides the mass hierarchy discrimination, JUNO has a rich physics program including a high-precision measurement of oscillation parameters, supernova neutrinos and geo-neutrinos [8].

REFERENCES

[1] Double Chooz Collaboration (Abe Y. *et al.*), *Phys. Rev. Lett.*, **108** (2012) 131801.
[2] Daya Bay Collaboration (An F. P. *et al.*), *Phys. Rev. Lett.*, **108** (2012) 171803.
[3] RENO Collaboration (Ahn J. K. *et al.*), *Phys. Rev. Lett.*, **108** (2012) 191802.
[4] DUNE Collaboration (Acciarri R. *et al.*), arXiv:1512.06148 [physics.ins-det].
[5] Abe K. *et al.*, arXiv:1109.3262 [hep-ex].
[6] KM3NeT Collaboration (Katz U. F.), arXiv:1402.1022 [astro-ph.IM].
[7] IceCube PINGU Collaboration (Aartsen M. G. *et al.*), arXiv:1401.2046 [physics.ins-det].
[8] JUNO Collaboration (An F. *et al.*), *J. Phys. G*, **43** (2016) 030401.
[9] Kim S. B., *Nucl. Part. Phys. Proc.*, **265-266** (2015) 93.
[10] Zhan L., Wang Y., Cao J. and Wen L., *Phys. Rev. D*, **79** (2009) 073007.
[11] T2K Collaboration (Abe K. *et al.*), *Nucl. Instrum. Methods A*, **659** (2011) 106.
[12] NOvA Collaboration (Patterson R. B.), *Nucl. Phys. Proc. Suppl.*, **235-236** (2013) 151.
[13] OPERA Collaboration (Agafonova N. *et al.*), *New J. Phys.*, **13** (2011) 053051.